# Development of Different Polymer Media and Experimental Investigation of Abrasive Flow Machining Process

**Sachin Dhull[1], R S Walia[2],  Q Murtaza[3], M.S.Niranjan[4]**

[1]*Research scholar,* [2,3,4]*Professor, Delhi Technological University, Delhi, India.*

**Abstract**

Abrasive Flow Machining is basically finishing process of internal passages using the flow of abrasive laden polymer media  with the help of extrusion pressure. In the paper, the different polymer media viz. styrene butadiene rubber, nitrile and natural rubber based media has been developed and subsequently the XRD and FTIR analysis has been done and experimentation has been performed on abrasive flow machine so as to calculate material removal rate and improvement in surface roughness has been analysed graphically.

**Keywords:** AFM, media, MRR

## 1. INTRODUCTION TO ABRASIVE FLOW MACHINING PROCESS AND THE POLYMER MEDIA USED

This paper combined the neural network approach with genetic algorithms to model and optimize the deposition of two polymers: diethylene glycol dimethacrylate and bisphenol A ethoxylate. Thickness, uniformity, modulus, and hardness were modeled, and optimum recipes were identified [1]. In this research, the mechanical strength of different SR composites before and after pyrolysis is studied. The big differences in volume variation between 650 C and 950 C suggests that the molten frits not only keep the shape of residual integrity but also react with around fillers and pyrolysis products at 950 C, resulting in obvious volume shrinkage [2].SEM images and XRD analysis reveal that amorphous SiO2 phase had transformed into cristobalite at 950 C, which has a significant effect on mechanical strength of the residues. The peak intensity of the emission band of NBR is more intense than that of SBR below 160 C, but less intense above 180 C. The peak intensity of the emission bands of H-NBR increases as the iodine value increases, strongly indicating that CL is caused by oxidation of double bonds in rubbers and that oxidative degradation can be monitored

effectively using CL spectral analysis [3]. It has been established by the RSM that the interaction between OPA and AMPTES in SBR compounds is consistent with the microstructure of the samples. The incorporation of OPA and AMPTES into SBR compounds enhances their compatibility, and thus improves their rheological properties [4].In this study, the coefficient of determination (R2) was sufficient to represent the model fit between the experimental and predicted values by the software. NCPE of MG49–LiCF3SO3–ZrO2/TiO2 sample films at different pH was successfully prepared in which zirconia and titania particles were produced via in-situ sol–gel technique and films by the solution casting method [5]. The observation on structural analysis showed the lowest degree of crystallinity was obtained at acid medium which also reflects the highest ionic conductivity value. A series of SBR composites filled with modified kaolin were prepared by melt blending. The kaolin layer-like particles presented significant characteristics with the diameter of 300 to 700 nm and the thickness of 50 to 150 nm in the composite matrix [6].The kaolin can reduce the gas permeability of the kaolin/SBR composite drastically, meantime, the reduction of particle size of kaolin and the increase of kaolin content in properly could improve the gas barrier property of the composite. In summary, we successfully prepared a PVDF/MVSR/FSR TPV by using FSR to improve the phase interfacial compatibility [7].The surfaces of some crosslinked rubber particles are connected by fiber-like elastomeric material which was originated from the light cured FSR. At last, the prepared PVDF/MVSR/FSR TPV shows the tensile strength and elongation at break of 9.5MPa and 200%, respectively. In summary, the electrochemical performance of the ZnFe2O4 electrodes prepared by the PVDF binder and the SBR/CMC binder has been investigated. In addition, it could provide an effective three-dimensional network with uniform distribution of the ZnFe2O4 active material and super P conductive additive. During charge discharge cycling, the SBR/CMC binder lowers the ohmic resistance of the electrode, depresses the formation of SEI film and facilitates the charge transfer reactions at the electrode/electrolyte interface. The fracture toughness value for a variety of pressureless-sintered ceramics and reaction-bonded ceramic composites was investigated through a four-point bend, chevron-notch technique. Digital image correlation was utilized to observe the presence of stable crack growth in quasi-static test specimens [8]. In general, it was determined that the presence of a residual silicon phase from the reaction bonding process improves the fracture toughness when compared to similar pressureless-sintered materials.

## 2. DEVELOPED MEDIA AND THEIR XRD AND FTIR IMAGES:

The commercially available abrasive media are very expensive and its affordability is an issue especially for price sensitive industries. Lower cost alternative AFM media are developed which consists of base polymers, additives and liquid plasticizer by uniformly mixing them to become the flexible mass. In the present experimental endeavor, an attempt is made in the direction of developing new media based on viscoelastic carrier.

### 2.1.Preparation of polymers:

The preparation of all the polymers was done at "Two roll mill machine" facility in Shriram institute of industrial research, New Delhi. For preparing the flexible polymers mass, a fixed quantity of polymer is taken first and an appropriate quantity of plasticizer is added into it. This plasticizer is not added just all in once, rather it is added slowly and it is only added during the crushing and rolling of solid polymer in two roll mill machines. In order to prepare natural rubber polymer, 100 gm natural rubber is weighted. This natural rubber is available in the form of sheet.

### 2.2.Preparation of media:

Take 300 gram of polymer and 80 gram of gel and then it is mixed by hand properly. Then add 400 gram of Silicon Carbide and it is properly mixed with it. Thus the media is prepared. Other media i,e Natural Rubber, SBR Rubber, Nitrile Rubber and Natural Rubber are also prepared in similar manner, as shown in fig.1,2 and 3 respectively.

**Fig.1.** Natural Rubber based media          **Fig.2.** Styrene Butadiene Rubber based media

**Fig.3.** Nitrile rubber based media

### 2.3.X-Ray Diffraction methods and images:

The X-Ray Diffraction (XRD) method is used for the phase confirmation of the component whose XRD is to be done. In the XRD machine, the light comes from the source, which falls on the component, then ultimately deflects at an angle $2\theta$ and

ultimately falls on the detector plate. The principle of operation is thermionic emission. In case of crystalline material, good peaks are observed in XRD images.
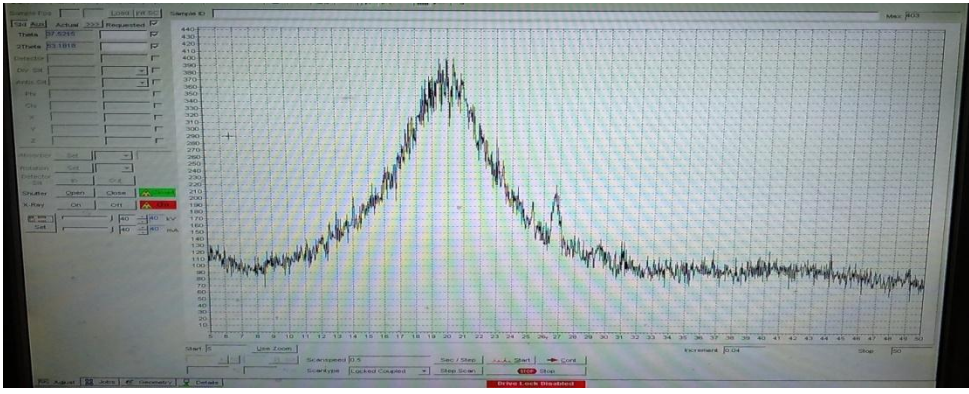


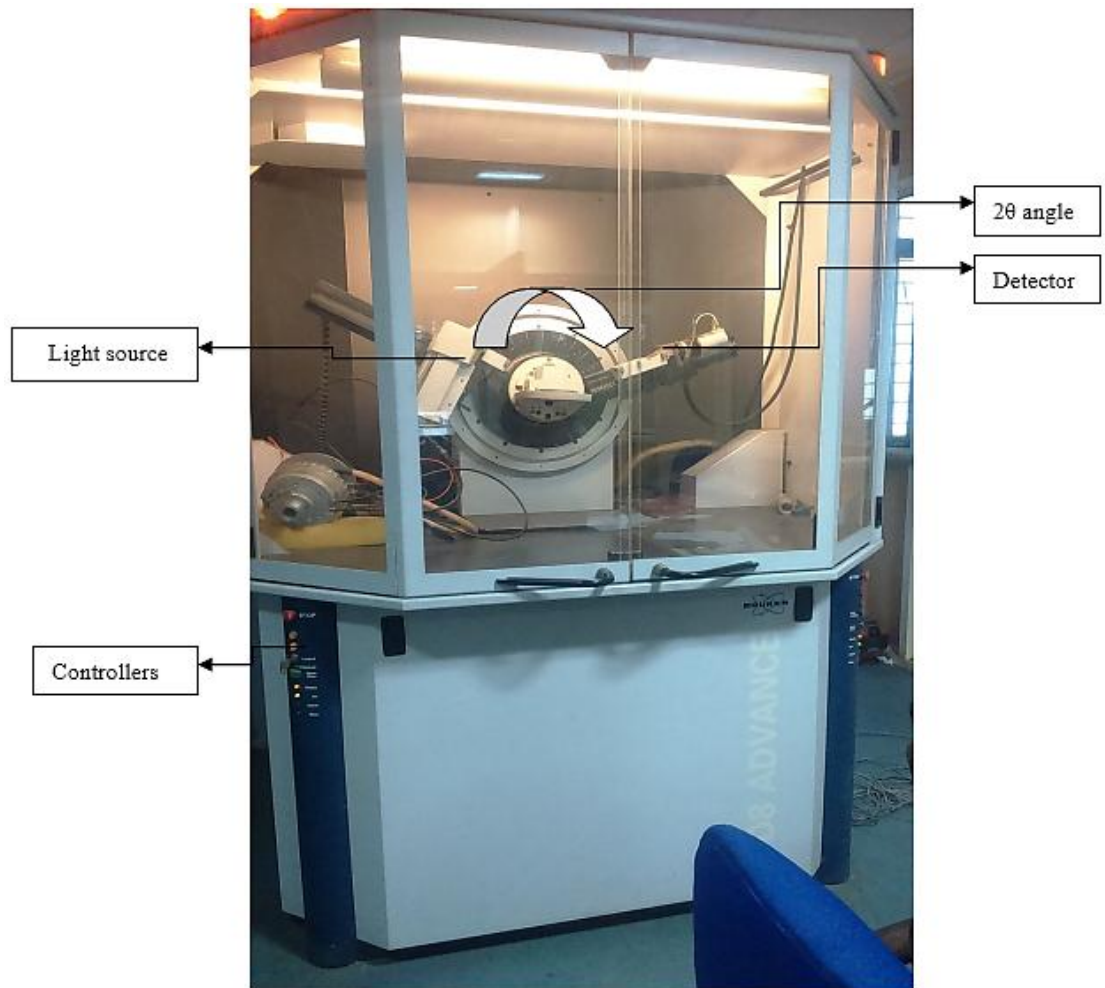**Fig.4.** X-Ray Diffraction image of  Nitrile Rubber based polymer media



**Fig.5.** Bruker X-Ray Diffraction Machine (D-8 Advance)

Different softwares are used for analysis of these images such as High Score, Origin and Xpertise, etc. Fig.5. shows Bruker X-Ray Diffraction Machine (D-8 Advance). The particle size i.e. diameter d can be calculated using:

$$d = \frac{0.9\, \beth}{\beta \cos\theta} \qquad\qquad (1)$$

where $\beth$ is the wavelength of light and $\beta$ is full width at half maximum, i.e. FWHM.
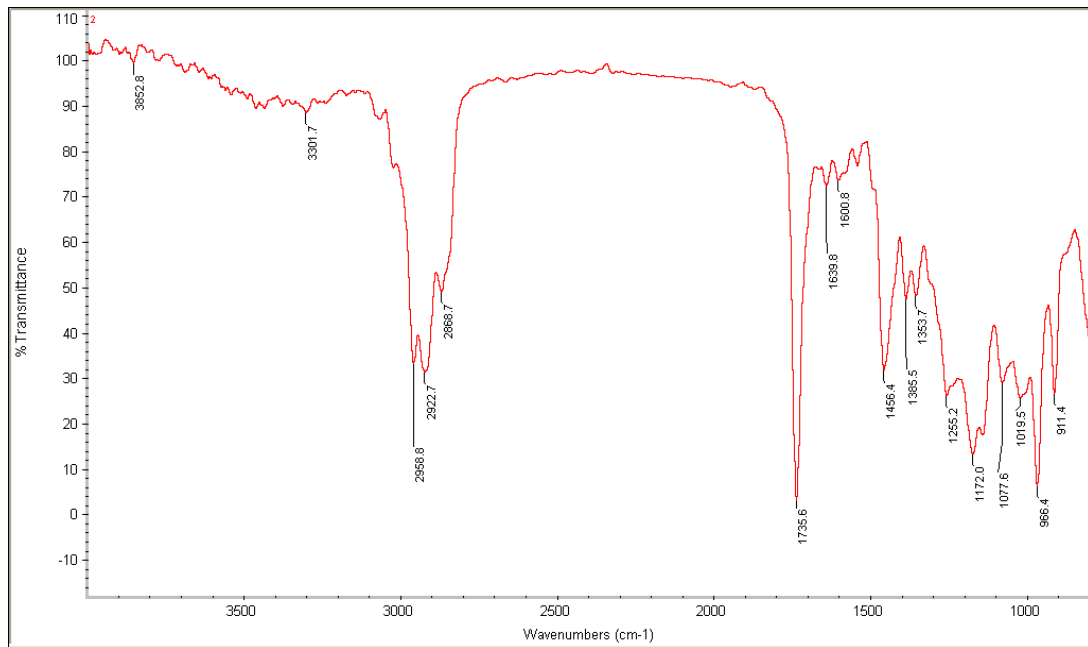


**Fig.6.** FTIR image of the developed Nitrile rubber media

The fig.6 clearly shows the FTIR image of nitrile polymer media i.e. transmittance vs wavenumber plot.

## 3. DEVELOPMENT AND DESIGN OF FIXTURE AND EXPERIMENTATION

The electrochemical based magnetic field assisted abrasive flow machining set up consists of three fixtures, made of nylon material. Dimensional analysis of the working AFM set up:

The distance travelled by magnetic force lines = workpiece thickness, A = 1 mm

The angle between the three solenoid electromagnets = 120º

The pole material is made of soft silicon iron, having better magnetic properties. It is cylindrical in shape.

### 3.1. Principle operation and charecteristics of the magnetic set up:

During the working operation, the magnetic lines of forces act towards the workpiece

whose internal wall surface has to be machined. In order to provide more focusing magnetic force towards the centre, the workpiece is placed inside the hollow cylindrical piece made of paramagnetic material, usually known as bright bar. The main aim of our model is to achieve high material removal and better morphological characteristics, which requires the development of electro-magnetic model. As the current supply to the developed solenoid arrangement is varied, the magnetic force gets changed. The following mathematical equations will predict the performance of abrasive flow finishing process.

### 3.1.1. Assumptions:

Taking all the parameters in electrochemical and magnetic force assisted AFM into account, the following assumptions are taken while writing mathematical equations:

(a)  The workpiece material is homogeneous and isotropic.
(b)  The magnetic field domain inside the workpiece is symmetrical about the axis.
(c)  Both cathode (cylindrical rod) and anode (workpiece) are conducting in nature.
(d)  The supply of current in the solenoid coils is assumed to be constant.
(e)  The magnetic abrasive particles are considered spherical- shaped.

### 3.1.2. Magnetic flux intensity and electrolytic force modeling:

The Maxwell equation (2)  is used to determine electromagnetic forces and the direction of the magnetic lines. The equation can be denoted mathematically as:

$$\nabla.B = 0 \tag{2}$$

where B is the magnetic flux density.

$$\frac{1}{r}\frac{d}{dr}\left(r\frac{d\varphi}{dr}\right) + \frac{d^2\varphi}{dz^2} = 0 \tag{3}$$

where $\varphi$ is the azimuthal angle, z is the height of the workpiece where the effect of magnetic field is produced.

According to British standard wire gauge: 19 gauge =  0.040 inch = 1.016 mm diameter

Resistance of 19 gauge wire = 0.0264 ohm/m, at 20 'C.

Copper density = 8.96 g/cm3 or 0.324 lb/in3

## 3.2. Fixture and electromagnet design and development:

The electromagnetic and magnetic assisted AFM utilizes fixture to hold workpiece, that results in improved material removal, which are shown in fig.7 to 9.
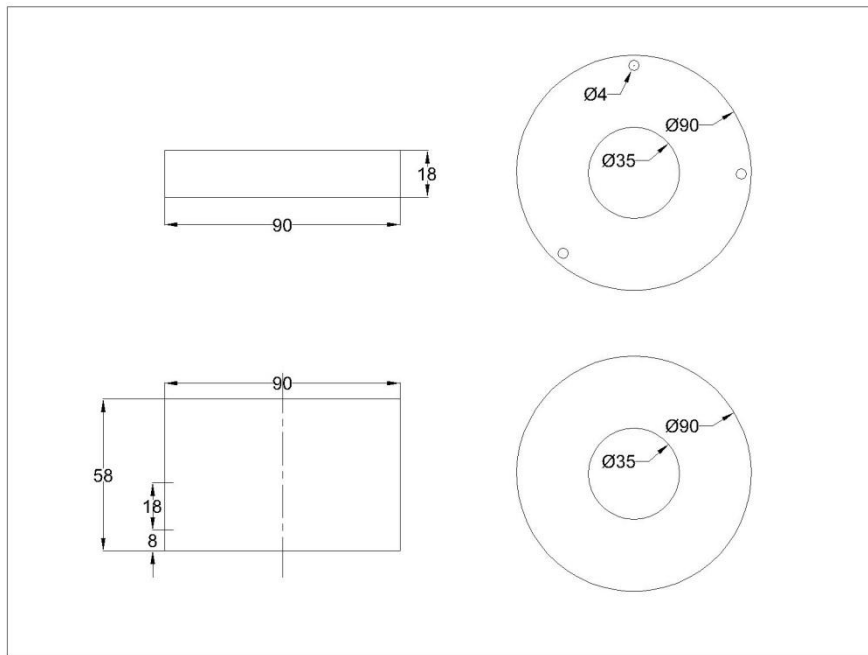
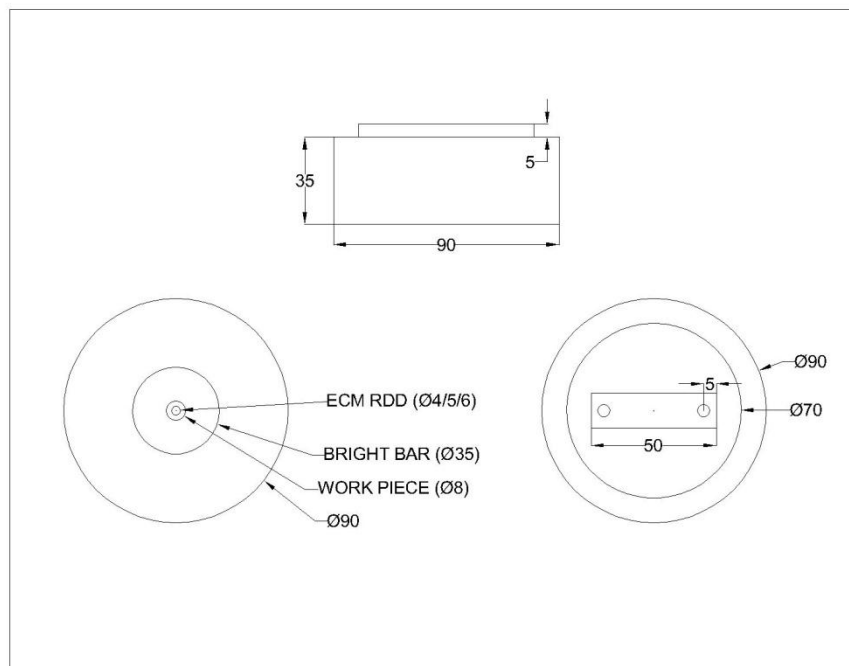**Fig.7.** Developed electrochemical and magnetic assisted AFM fixture
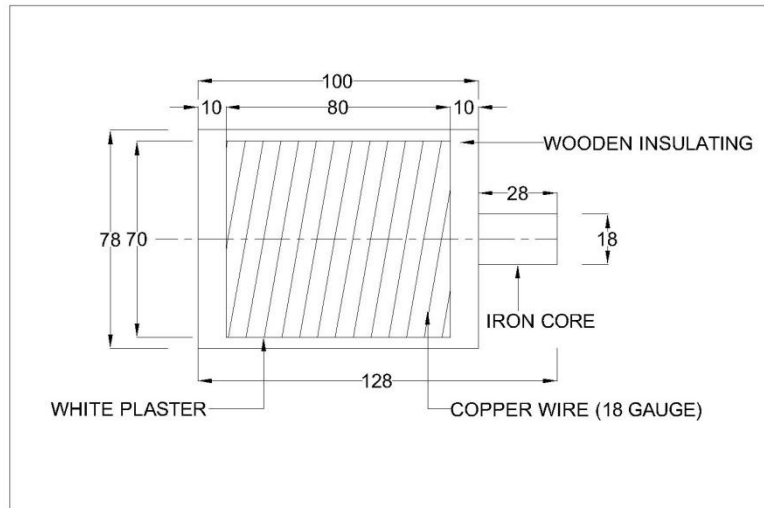


**Fig.8.** Top view of the fixture

**Fig.9.** Developed electromagnetic solenoid design

### 3.3. Experimental results of material removal:

During abrasive flow machining, three parameters viz. extrusion pressure, number of cycles and abrasive mesh size were taken and their effect on material removal is graphically shown in fig. 10 to 12. In fig.10, material removal first increases, reaches maximum at pressure of 22 bar and then decrease with increase in pressure. The same effect is shown in case of increase of number of cycles. In case of abrasive mesh size, it is shown in fig.12 that the material removal continuously decreases with increase in mesh size.
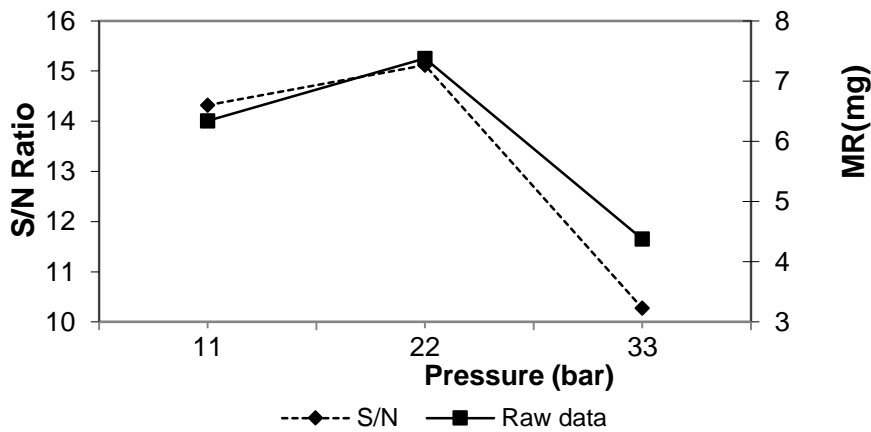


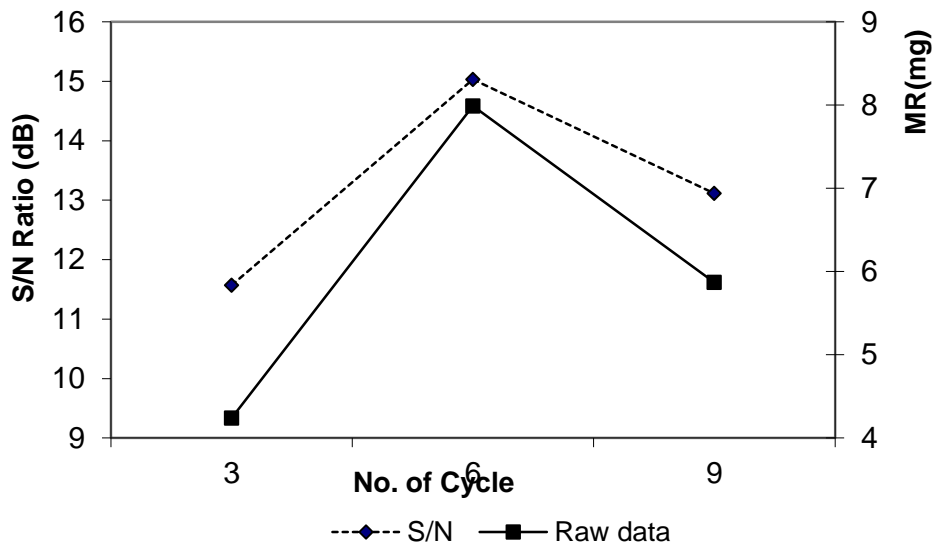**Fig.10.** SN Ratio graph showing material removal vs pressure plot

**Fig.11.** SN Ratio graph showing material removal vs number of cycles plot
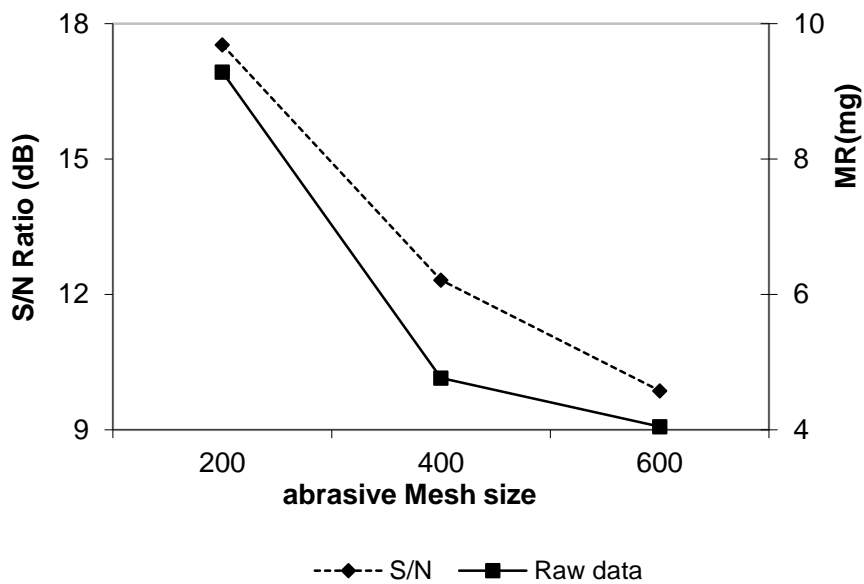


**Fig.12.** SN Ratio graph showing material removal vs abrasive mesh size plot

## 4. CONCLUSION

In the paper, the three different polymer media are developed viz. Nitrile, Styrene Butadiene and natural rubber and the experimental work is performed on the developed electrochemical and magnetic assisted abrasive flow machining nylon

fixture. The X-Ray diffraction and FTIR analysis of the media is also done. The material removal first increases, reaches maximum at pressure of 22 bar and then decrease with increase in pressure. The same effect is shown in case of increase of number of cycles which has been clearly shown graphically.

## REFERENCES

[1] Edem Wornyo, Gary S. May, Ken Gall, "Modeling and Optimization of the Deposition of Shape Memory Polymers for Information Storage Application"

[2] Jinhe Wang, Chentao Ji, Yuantao Yan, Di, 2015, "Mechanical and ceramifiable properties of silicone rubber filled with different inorganic fillers", Polymer Degradation and Stability 121, pp.149e156

[3] Chikahiro Satoh , Hiroshi Ishii , Masatake Hasumi , Emi Yamada , Keith R. Millington, Munetaka, 2015, "Chemiluminescence spectral analysis of styrene-butadiene and acrylonitrile-butadiene rubbers using a multichannel Fourier-transform chemiluminescence spectrometer, Polymer Testing 43, pp.44e48

[49] Zhong Xian Ooi, Hanafi Ismail, 2015, "Interaction between 3-amino propyl trimethoxy silane and oil palm ash in styrene butadiene rubber compounds using response surface methodology", Polymer Testing 43, pp. 131e138

[5] L. TianKhoon , N.H. Hassan, M.Y.A. Rahman, "One-pot synthesis nano-hybrid ZrO2–TiO2 fillers in 49% poly(methylmethacrylate) grafted natural rubber (MG49) based nano-composite polymer electrolyte for lithium ion battery application"

[6] Yinmin Zhang , Qinfu Liu , Shilong, 2015, "Gas barrier properties and mechanism of kaolin/styrene–butadiene rubber nanocomposites", Applied Clay Science 111, pp.37–43

[7] Chuanhui Xu, Yanpeng Wang , Baofeng, 2015, "Thermoplastic vulcanizate based on poly(vinylidene fluoride) and methyl vinyl silicone rubber by using fluorosilicone rubber as interfacial compatibilizer", Materials and Design 88, pp.170–176

[8] Rongyu Zhang , Xu Yang , Dong Zhang , Hailong Qiu, 2015, "Water soluble styrene butadiene rubber and sodium carboxyl methyl cellulose binder for ZnFe2O4 anode electrodes in lithium ion batteries", Journal of Power Sources 285, pp.227e234